Kinesin's tail domain is an inhibitory regulator of the motor domain

David L. Coy*, William O. Hancock*, Michael Wagenbach* and Jonathon Howard*†

*Department of Physiology & Biophysics, University of Washington, Box 357290, Seattle, Washington 98195-7290, USA
†e-mail: johoward@u.washington.edu

When not bound to cargo, the motor protein kinesin is in an inhibited state that has low microtubule-stimulated ATPase activity. Inhibition serves to minimize the dissipation of ATP and to prevent mislocalization of kinesin in the cell. Here we show that this inhibition is relieved when kinesin binds to an artificial cargo. Inhibition is mediated by kinesin's tail domain: deletion of the tail activates the ATPase without need of cargo binding, and inhibition is re-established by addition of exogenous tail peptide. Both ATPase and motility assays indicate that the tail does not prevent kinesin from binding to microtubules, but rather reduces the motor's stepping rate.

Kinesin is a motor protein that is essential for the microtubule-based transport of membrane-bound organelles in neurons and other cells[1–4]. However, despite the extensive characterization of kinesin *in vivo* and *in vitro*[5], the mechanism by which this protein sorts organelles to appropriate cellular locations is poorly understood. Precisely which organellar cargo does kinesin move? What regulates the loading of the cargo onto the motor? And how is the motor switched on after the cargo is loaded? It is the last question that we address here.

Kinesin's motor and ATPase activities must be tightly coupled to the binding and transport of cargo, for several reasons. First, if kinesin were active when not bound to cargo, then the 0.1–1 μM kinesin found in tissues[6], each molecule of which is hydrolysing ~100 ATP molecules per second (ref. 7), would squander a large amount of ATP, equivalent to 10–100 μM ATP per second, an amount comparable to the basic metabolic rate of humans (~100 kJ kg^{-1} day^{-1}; ref. 8). A second, potentially more serious problem is that unregulated cargo-free kinesin would walk processively along a microtubule from the minus end, where it is needed for loading cargo, to the plus end where it can serve no useful purpose as it would be at the end of the road. For these reasons, it is important that kinesin be inhibited when cargo-free and switched on only after binding cargo. Consistent with such tight regulation, kinesin purified from native sources has a very low microtubule-stimulated ATPase rate of ~1 ATP per second (refs 9, 10).

An understanding of how the ATPase and motor activities of kinesin might be regulated requires knowledge of the domain organization of the molecule (Fig. 1a,b). Kinesin consists of two identical heavy chains that dimerize through the formation of several parallel coiled-coil domains[11–14] to form a homodimer, α_2. At the amino terminus is the 'head', a motor domain[15] that contains the ATP- and microtubule-binding sites[16]. The next ~600 amino acids are predicted to form a series of coiled-coils separated by more flexible regions. The carboxy-terminal third of this region mediates binding of two light chains[17–19]. The last ~60 amino acids form a small, positively charged globular domain; this small 'tail', perhaps in conjunction with the two identical light chains (β_2), probably mediates kinesin binding to specific membrane-bound organelles such as vesicles[2,20,21].

Crucial insight into how the motor might be regulated came from electron-microscopic observations and hydrodynamic measurements showing that, under normal ionic conditions, native kinesin is flexed with its head and tail domains in close proximity[10,22]. It was proposed that the tail might bind to and inhibit the heads, thereby inactivating this flexed enzyme. This tail-inhibition model (Fig. 1c), which is analogous to that proposed for the regulation of smooth-muscle myosin[23,24], accounts for the low ATPase activity of native kinesin mentioned above and the high ATPase activity of proteolysed and truncated, tail-less kinesins[13,25,26].

Several predictions can be made on the basis of the tail-inhibition model for kinesin regulation. First, the binding of a cargo to the full-length protein is expected to interfere with the interaction of the tail and the head, and so should result in activation of the ATPase activity[22,27]. Second, deletion of the tail domain or prevention of head–tail interactions should also activate the ATPase.

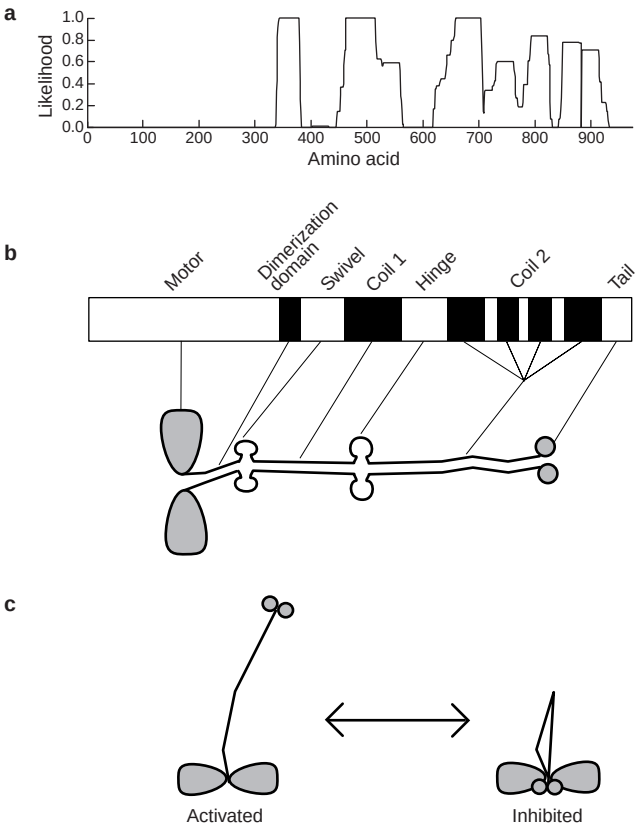

Figure 1 **Structural model for kinesin and its regulation. a**, Likelihood of each amino acid of the *Drosophila* kinesin heavy chain being part of a coiled-coil according to the Paircoil program[32]. **b**, Structural model of kinesin based on known structures of the head and dimerization domain[14] and the structure prediction in **a**. **c**, Tail-inhibition model for the regulation of kinesin; this model postulates that the motor is active in the extended (open) conformation and inactive in the flexed (closed) conformation.

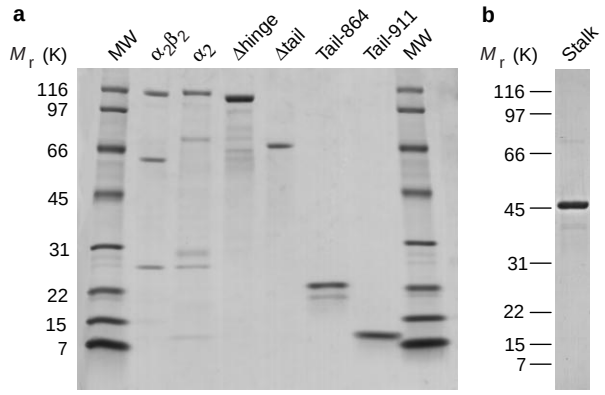

Figure 2 **Coomassie-stained SDS–polyacrylamide gels of wild-type and mutant kinesin proteins. a**, MW, molecular-mass standard; $\alpha_2\beta_2$, recombinant wild-type kinesin consisting of two heavy and two light chains; α_2, kinesin heavy-chain homodimer; Δhinge, kinesin heavy chain lacking residues S560–D624; Δtail, kinesin heavy chain deleted after residue M559; tail-864, a kinesin-heavy-chain construct consisting of amino acids 864–975; tail-911, a kinesin-heavy-chain tail construct consisting of amino acids 911–975. **b**, Stalk, residues 368–685 of the kinesin heavy chain.

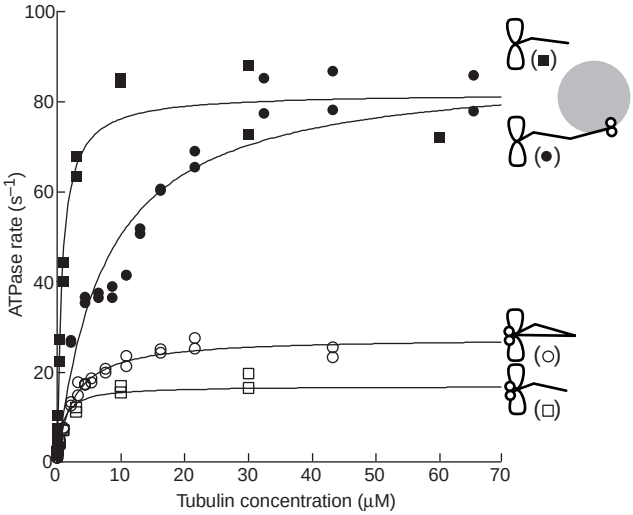

Figure 3 **Kinesin's ATPase rate is activated by cargo binding or by deletion of its tail domain.** In solution, full-length kinesin, α_2, has a low microtubule-stimulated ATPase rate (open circles) that is activated by artificial transport cargo consisting of 200-nm casein-coated silica beads (filled circles; the bead is represented by a large grey circle). Deletion of the tail domain (Δtail kinesin) also activates the ATPase rate (filled squares) to a similar extent and activation is reversed by the addition of 10 mM exogenous tail peptide (tail-911, open squares). Lines represent Michaelis–Menten fits to the data as described in the Methods. Figures represent hypothetical kinesin structures.

Third, addition of exogenous tails should inhibit both ATPase and motor activities. We test these predictions here.

Results

To test the kinesin tail-inhibition model, we measured the microtubule-stimulated ATPase activity of full-length recombinant *Drosophila* kinesin and kinesin mutant constructs (Fig. 2) in the presence and absence of exogenous kinesin tail peptides.

Cargo-activated ATPase activity. The microtubule-stimulated ATPase rate of recombinant full-length kinesins was activated three- to sevenfold by binding to an artificial cargo (Table 1). In solution (that is, when not bound to cargo), the maximal microtubule-stimulated ATPase rate, k_{cat} (the number of ATPs hydrolysed per second per molecule), was 28±2 s^{-1} for kinesin homodimer α_2 (mean±s.e.m., Fig. 3). By contrast, when this kinesin was adsorbed to 200-nm-diameter glass beads at <1 motor per bead, k_{cat} increased to 88±6 s^{-1} (Fig. 3). The ATPase rate of heterotetrameric kinesin, $\alpha_2\beta_2$, which contains the two light chains in addition to the heavy chains, was activated to the same level by bead binding (Table 1). The ATPase rate of $\alpha_2\beta_2$ in the absence of beads was lower than that of α_2 but was still significant. We do not believe that the non-zero ATPase rate of $\alpha_2\beta_2$ in solution is due to contamination by α_2 (see Methods), but rather that the light chains have an additional modulatory effect on the ATPase rate.

We confirmed that the beads did indeed act as cargoes by observing their movement along microtubules, using differential interference contrast microscopy[7]. Cargo binding activated kinesin to its maximal level: comparing the speed of movement (~600–800 nm s^{-1}) with the bead-activated k_{cat} (~80–100 s^{-1}) indicates that, under these single-molecule conditions, both α_2 and $\alpha_2\beta_2$ kinesin take one 8-nm step per ATP hydrolysed[7].

To determine whether the kinesin tail domain is necessary for inhibition, we tested Δtail, a kinesin construct truncated after amino acid M559 (Fig. 2). Its microtubule-stimulated ATPase rate of 81±6 s^{-1} was similar to that of cargo-activated kinesin (Fig. 3, Table 1). To ensure that the activation was due to the absence of its tail, we measured the ATPase activity of Δtail in the presence of an exogenous kinesin tail fragment, tail-911, which comprises amino acids 911–975. Addition of 10 μM tail-911 decreased the k_{cat} of Δtail to 17±2 s^{-1}, comparable to the ATPase rate of α_2 in the absence of beads (Fig. 3). Thus, consistent with the results obtained from study of α_2 in solution, the tail peptide alone, without need for light chains, is sufficient to inhibit the ATPase. As a control against non-specific inhibition by tail-911, we tested an expressed fragment of the kinesin stalk, residues 368–685, which includes neither the head nor the tail domain; this fragment had no effect on the ATPase rate of Δtail (data not shown).

We measured the ATPase rate of Δtail kinesin in the presence of 20 μM polymerized tubulin over a wide range of tail-peptide concentrations (Fig. 4a). The results indicate that the tail-mediated

Table 1 Steady-state ATPase rates of activated and inhibited kinesins

Inhibited form			Activated form		
Species	**k_{cat}*(s^{-1})**	**K_m† (μM)**	**Species**	**k_{cat} (s^{-1})**	**K_m (μM)**
α_2 in solution	28±2	3±1	α_2 + beads	88±6	7±1
$\alpha_2\beta_2$ in solution	12±1	2±1	$\alpha_2\beta_2$ + beads	88±10	15±3
Δtail + 10 μM tail-911	17±2	0.9±0.3	Δtail	81±6	0.7±0.1
Δhinge + 12 μM tail-911	28±2	3.0±0.5	Δhinge	79±9	11±2

* k_{cat} refers to the rate of ATP hydrolysis per kinesin dimer. Errors are ±s.e.m. from fits to data.
† K_m refers to the concentration of polymerized tubulin to half-maximally stimulate the ATPase activity.

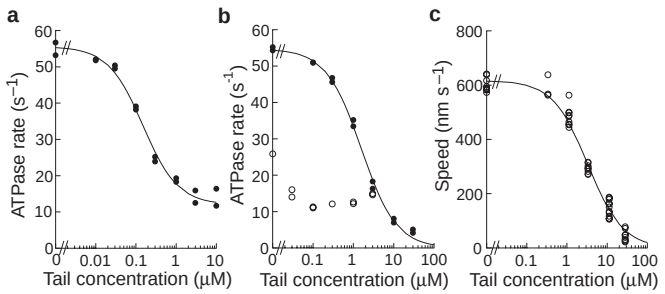

Figure 4 **Exogenous kinesin tail protein inhibits kinesin's ATPase activity and motility.** The effect of tail-911 peptide on **a**, the ATPase rate of Δtail at 20 μM polymerized tubulin; **b**, the ATPase rate of α_2 bound to beads (filled circles) and in solution (open circles) at 10 μM and 15 μM polymerized tubulin, respectively; and **c**, the microtubule-gliding speed of α_2. K_i = 0.15 μM for the ATPase rate of Δtail, 1.6 μM for the ATPase rate of cargo-activated α_2, and 3.3 μM for the gliding speed of α_2.

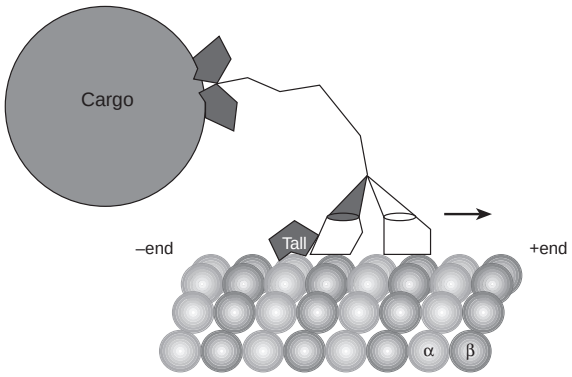

Figure 5 **A structural model of tail-mediated inhibition.** The kinesin tail promotes formation of a trimolecular complex (consisting of kinesin head, microtubule, represented here by spheres labelled with α and β, and kinesin tail) that slows the detachment of the trailing head from the microtubule, thereby slowing the stepping frequency. Formation of a trimolecular complex is not strictly necessary: if the binding of the tail to the head interferes with the coordinated motion of the two heads in such a way as to prevent one head from accelerating the release of the other head, then hand-over-hand motility will be impeded. Microtubule plus and minus ends are indicated.

inhibition is not cooperative—the binding of only one tail molecule suffices for inhibition. The concentration of tails producing half-maximal inhibition of ATPase activity, K_i, was 150±20 nM (mean±s.e.m.). Interestingly, the ATP-hydrolysis rate of Δtail was not fully inhibited by the tail peptide: there is a clear saturation at ~18% of the maximum activity. Even though tail-911 bound to microtubules in pelleting assays (dissociation constant <1 μM, using the method of ref. 28), complete decoration of the microtubule was not necessary for inhibition: half-maximal inhibition of the ATPase rate was obtained at a tail concentration that is 130-fold lower than the tubulin concentration present in these assays.

In addition to inhibiting Δtail kinesin, tail-911 inhibited full-length kinesin in both the presence and the absence of cargo (Fig. 4b). Similar to the results obtained with Δtail, α_2 in solution could not be fully inactivated.

The tail inhibits motility. Tail-911 completely inhibits motility in microtubule gliding assays. Following infusion of buffer containing tail-911 into a flow cell, microtubules continued to move continuously without pauses or stops, but their gliding speed decreased (Fig. 4c). At saturating tail concentrations movement was completely arrested, resulting in fields containing large numbers of immobile microtubules. Half-maximal inhibition occurred at a concentration of 3.3 μM. Similar inhibition was also obtained with a longer, dimeric tail peptide, tail-864. Tail-911-mediated inhibition of microtubule motility was fully reversible and was similar at 1 mM and 10 mM ATP.

The higher concentration of tail needed to inhibit the motility as compared with the ATPase activity probably results from loss of tail to the glass surfaces. The binding capacity of the casein-coated beads, measured in centrifugation studies, is 6,000 tail-911 molecules per bead, corresponding to a density of $50\times10^3\,\mu m^{-2}$. The surface-to-volume ratio of the flow cells used for the motility experiments is such that a complete surface coating of tail-911 would require a few micromolar of tails, so the true K_i for the motility could be significantly lower. Even though the tail does bind to the surface of flow cells, it is unlikely that inhibition of motility is due to crosslinking of microtubules to the flow-cell surface. First, even saturating the surface with tails did not promote microtubule adhesion in the absence of motors. Second, at a given tail concentration the inhibition of motility was not dependent on the surface density of motors—if inhibition were due to a 'braking' mechanism, then we would expect inhibition to be stronger at lower motor densities when fewer motors would be available to overcome the brake.

Several observations indicated that tail-911 promotes the association between kinesin and microtubules in the motility assay. For example, in the presence of 5.6 μM tail-911, the speed of α_2 was reduced to 44% of control. The tails had no significant effect on either the rate at which microtubules bound to the surfaces (landing rates of 20±4 $mm^{-2}\,s^{-1}$ versus 19±4 $mm^{-2}\,s^{-1}$ with and without tails respectively; kinesin density equal to 10 motors μm^{-2}) or the average distance moved before dissociating (9 μm with tails and 7 μm without). However, the time spent moving on the surface was significantly longer in the presence of tails (29 s with tails and 10 s without tails, for 20 and 19 observed dissociations, respectively), reflecting the lower speed in the presence of tails.

Inactivation of kinesin requires the hinge region. The tail-inhibition model outlined above postulates that kinesin flexes about a molecular hinge to allow the tails to inhibit the motor domains. To test this hypothesis, we deleted the putative hinge region that was shown by electron microscopy to be the likely site of flexion[22,29,30]. Deletion of amino acids S560–D624 created a kinesin, Δhinge, that was predicted to have a high likelihood of forming a continuous, in-register coiled-coil by the Coils[31] and Paircoil[32] programs. As predicted by the tail-inhibition model, the microtubule-stimulated ATPase rate of Δhinge was high—the k_{cat} of 79±9 s^{-1} was comparable to that of cargo-activated α_2 (Table 1). To confirm that the activated ATPase rate of Δhinge resulted from a disruption of tail-mediated inhibition, we repeated the ATPase measurement in the presence of 12 μM tail-911 protein; the k_{cat} of Δhinge fell to 28±2 s^{-1}, a level similar to that of α_2 in the absence of cargo-binding (Table 1).

To assess whether deletion of the putative hinge disrupts tail-mediated inhibition by maintaining kinesin in its extended state, we measured the sedimentation coefficient of Δhinge and compared it with those of the flexed and extended conformations of α_2. The sedimentation coefficient of α_2 was 6.8–7.2S (data not shown and ref. 33), similar to that of native dimeric kinesin, which has been shown by electron microscopy to be flexed[22]. In 1 M NaCl, which disrupts the head–tail interaction and results in kinesin taking on an extended form[22], the sedimentation coefficient was 5.9±0.4S. In BRB80 buffer the sedimentation coefficient of Δhinge was 7.8±0.1S. This was surprising: instead of having a lower sedimentation coefficient than α_2 in the extended conformation, as expected (a lower molecular weight and a similar shape should give a lower sedimentation coefficient), Δhinge had a higher sedimentation coefficient than α_2 in the flexed conformation. Rather than interpreting this result as Δhinge being in an even more compact conformation than that of flexed α_2, we think instead that Δhinge has probably

tetramerized. Indeed, an antiparallel dimer of dimers, with the head of each molecule binding to the tail of the other, is predicted by the tail-inhibition model shown in Fig. 1c. Consistent with this interpretation, modelling of the sedimentation coefficient of such a Δhinge tetramer using the approach of ref. 34 gave a predicted sedimentation coefficient of 8.0S. Thus, although we expect, on the basis of sequence analysis, that Δhinge has an extended conformation, our attempts to verify this produced ambiguous results.

Discussion

We have shown that a 65-amino-acid C-terminal 'tail' domain is an inhibitory regulator of the ATPase and motor activities of kinesin's head domains. The strongest evidence for this proposal is that deletion of the tail activates the ATPase rate, and addition of exogenous tail reverses this activation and inhibits motility. Because the activation is mimicked by binding of full-length kinesin to cargo (and reversed by addition of exogenous tail), we propose that the binding of cargo antagonizes tail inhibition, thereby switching the motor on. Cargo-mediated activation is consistent with the tail-inhibition model proposed in ref. 22 and shown in Fig. 1c, because it is expected that the binding of kinesin to a bead would interfere with the flexing of the molecule. Likewise, the activation of the ATPase activity by removal of a putative hinge region is also consistent with this model. However, our results do not distinguish between models in which the tail interacts directly with the motor domain and those in which the tail binds outside the motor domain and inhibits allosterically.

Several observations indicate that the tail-mediated inhibition is not due to a steric blocking mechanism. If the tail were to sterically block the head from binding to microtubules, it would act as a competitive inhibitor: the maximal microtubule-stimulated ATPase rate (k_{cat}) for inhibited kinesin would not be lower than that for activated kinesin, and instead the microtubule concentration required for half-maximal stimulation of ATPase activity (K_m, expressed as tubulin-dimer concentration) would be increased (see, for example, ref. 35). This is clearly not the case: inhibition of kinesin, either by adding tail peptides or by taking away beads, always resulted in a lower k_{cat} and never caused an increase in the K_m (Table 1). Hence, the kinesin tail must be inhibiting the motor by a mechanism other than a steric block of microtubule binding.

A simple model that accounts for our data is that the tail decreases the rate at which kinesin steps along the microtubule (Fig. 5). This is in agreement with the decrease in speed observed when tails are added to motility assays. If each step is associated with the hydrolysis of one molecule of ATP, as is the case under normal, fully activated, conditions[7], then a decrease in stepping rate would lead to the observed decrease in k_{cat}. Furthermore, if the distance moved is not affected by the tail, again in accordance with the gliding assays, then the lower speed will result in a reduced kinesin off-rate and therefore a lower K_m for the microtubule-mediated stimulation of the ATPase, as we observed. This model also assumes that the kinesin on-rate is not changed, consistent with the tails not affecting the rate at which microtubules bind to the kinesin-coated surfaces used in the motility assays.

The tail-inhibition model does not rule out a potentially important regulatory role for phosphorylation[36,37] or other covalent modification in regulation of kinesin activity. Rather, the tail-inhibition model and our data fit nicely with the existence of extra regulatory mechanisms. We expect that *in vivo* regulation of kinesin activity would be greater than the three- to sevenfold level we measured for the bacterially expressed protein. During our initial studies we found that the level of cargo-mediated activation of kinesin purified from native sources was greater than that of the recombinant proteins. We have also noted previously that the motor activity of native protein is typically ten times less than that of recombinant protein (see, for example, ref. 33). These observations all indicate that native kinesin may be regulated by other means not detected in our bacterial expression system. It is likely that the kinesin light chains are an important target for this regulation, given that they markedly influence the binding of kinesin to microtubules when expressed in COS cells[19]. We are now exploring these possibilities, as well as the hypothesis that other regulatory mechanisms modulate the folding and/or inhibition by the tail. □

Methods

Preparation of kinesin constructs.

All kinesin constructs were derived from the wild-type, full-length *D. melanogaster* kinesin heavy chain gene[7]. DNA-propagation steps were done in *Escherichia coli* strain DH5a or CJ236 with final placement in pET vectors. Enzymes were purchased from New England BioLabs, except T4 DNA ligase (Gibco) and T4 gene 32 protein (Boehringer Mannheim). Each kinesin construct was expressed as a C-terminally His-tagged fusion protein unless otherwise stated. Heterotetrameric kinesin ($\alpha_2\beta_2$) contained an untagged heavy chain (α) and a tagged light chain (β). Δtail kinesin consists of α_2 truncated after residue M559. To create Δhinge kinesin, we deleted the sequence coding for amino acids S560–D624 from the His-tagged α_2 construct. Tail-911 protein contains the terminal 65 amino acids of kinesin heavy chain joined to an N-terminal His tag. A kinesin stalk peptide comprised amino acids 368–685.

Protein expression and purification.

Proteins were bacterially expressed and purified by Ni-NTA agarose affinity chromatography as described[7] (Fig. 2). The motor-containing kinesin constructs were further purified by phosphocellulose (Whatman) chromatography. $\alpha_2\beta_2$ kinesin contains negligible α_2 because the latter is not His tagged and does not bind to Ni-NTA. Analysis of phosphocellulose-purified $\alpha_2\beta_2$ by Coomassie-stained SDS–PAGE revealed a light-chain:heavy-chain ratio of 1.3–1.5:1 (ref. 7). Tail-911 was concentrated and further purified by SP Sepharose (Pharmacia) chromatography after dialysing into 50 mM imidazole, 100 mM NaCl, 2 mM EDTA, 2 mM $MgCl_2$, 5 mM dithiothreitol, pH7.0. The protein was eluted in a linear gradient of sodium chloride (0.1–1.0 M) in the same buffer, and moved into BRB80 buffer by passage through a PD-10 column containing G-25M Sephadex (Pharmacia). Buffers were augmented with 50–100 μM Mg-ATP. All proteins were frozen in liquid nitrogen, and stored at –80 °C.

The concentration of active motors was determined by radionucleotide binding[7] and expressed in terms of dimers. Adsorption of proteins to 0.2-μm silica beads had no effect on protein activity or accessibility to microtubules, as described[7]. The concentration of the tail-911 protein was quantified both by ultraviolet absorption and by scanning Coomassie-stained SDS–polyacrylamide gels.

During initial studies, tail-864, a longer tail construct that is predicted to form a coiled-coil, was tested. This protein crosslinked microtubules in motility and ATPase assays, consistent with it being a dimer. Tail-911 does not crosslink microtubules and preliminary NMR studies indicate that it is compact and monomeric (S. Sarma, M. Wagenbach, J. Howard and A. P. Campbell, unpublished observations).

Protein-sedimentation coefficients were determined by centrifugation through linear BRB80:sucrose gradients as described[33].

ATPase and motility assays.

Steady-state ATPase activity at 25±1 °C was measured in BRB80 buffer with 1 mM Mg-ATP, 10 μM Taxol, 1 mg ml^{-1} casein and a variable amount of Taxol-stabilized microtubules and kinesin using the malachite green assay[7]. The kinesin concentration ranged from 0.2 to 1 nM and the incubation times from 30 to 200 min, depending on the microtubule concentration. The turnover rates are expressed per kinesin molecule. Kinesin was adsorbed to 200 nm casein-coated silica beads at a ratio of 1:5 as described[7].

Speeds were determined in standard motility assays by observing rhodamine-labelled microtubules gliding over a motor-coated glass surface[38].

Plots of ATPase activity (per dimeric kinesin molecule) versus tubulin concentration were fitted to the Michaelis–Menten equation[35] using IgorPro (Wavemetrics, Lake Oswego, OR) as described[7].

RECEIVED 13 JANUARY 1999; REVISED 30 JUNE 1999; ACCEPTED 23 JULY 1999;
PUBLISHED 11 AUGUST 1999.

1. Hurd, D. D. & Saxton, W. M. Kinesin mutations cause motor neuron disease phenotypes by disrupting fast axonal transport in *Drosophila*. *Genetics* **144,** 1075–1085 (1996).
2. Coy, D. L. & Howard, J. Organelle transport and sorting in axons. *Curr. Opin. Neurobiol.* **4,** 662–667 (1994).
3. Bloom, G. S. & Endow, S. A. Motor proteins I: kinesins. *Protein Profile* **2,** 1109–1171 (1995).
4. Hirokawa, N. Kinesin and dynein superfamily proteins and the mechanism of organelle transport. *Science* **279,** 519–526 (1998).
5. Howard, J. Molecular motors: structural adaptations to cellular functions. *Nature* **389,** 561–567 (1997).
6. Hollenbeck, P. J. The distribution, abundance and subcellular localization of kinesin. *J. Cell Biol.* **108,** 2335–2342 (1989).
7. Coy, D. L., Wagenbach, M. & Howard, J. Kinesin takes one eight-nanometer step for each ATP that it hydrolyzes. *J. Biol. Chem.* **276,** 3667–3671 (1999).
8. Berne, R. M. & Levy, M. N. *Physiology* 3rd edn (Mosby, St Louis, 1993).
9. Saxton, W. M. *et al. Drosophila* kinesin: characterization of microtubule motility and ATPase. *Proc. Natl Acad. Sci. USA* **85,** 1109–1113 (1988).
10. Hackney, D. D., Levitt, J. D. & Wagner, D. D. Characterization of alpha 2 beta 2 and alpha 2 forms of kinesin. *Biochem. Biophys. Res. Commun.* **174,** 810–815 (1991).
11. Yang, J. T., Laymon, R. A. & Goldstein, L. S. A three-domain structure of kinesin heavy chain revealed by DNA sequence and microtubule binding analyses. *Cell* **56,** 879–889 (1989).
12. de Cuevas, M., Tao, T. & Goldstein, L. S. Evidence that the stalk of *Drosophila* kinesin heavy chain is an alpha-helical coiled coil. *J. Cell Biol.* **116,** 957–965 (1992).
13. Huang, T. G., Suhan, J. & Hackney, D. D. *Drosophila* kinesin motor domain extending to amino acid position 392 is dimeric when expressed in *Escherichia coli*. *J. Biol. Chem.* **269,** 16502–16507 (1994).
14. Kozielski, F. *et al.* The crystal structure of dimeric kinesin and implications for microtubule-dependent motility. *Cell* **91,** 985–994 (1997).

15. Kull, F. J., Sablin, E. P., Lau, R., Fletterick, R. J. & Vale, R. D. Crystal structure of the kinesin motor domain reveals a structural similarity to myosin. *Nature* **380,** 550–555 (1996).
16. Yang, J. T., Saxton, W. M., Stewart, R. J., Raff, E. C. & Goldstein, L. S. Evidence that the head of kinesin is sufficient for force generation and motility *in vitro*. *Science* **249,** 42–47 (1990).
17. Cyr, J. L., Pfister, K. K., Bloom, G. S., Slaughter, C. A. & Brady, S. T. Molecular genetics of kinesin light chains: generation of isoforms by alternative splicing. *Proc. Natl Acad. Sci. USA* **88,** 10114–10118 (1991).
18. Gauger, A. K. & Goldstein, L. S. The *Drosophila* kinesin light chain. Primary structure and interaction with kinesin heavy chain. *J. Biol. Chem.* **268,** 13657–13666 (1993).
19. Verhey, K. J. *et al.* Light chain-dependent regulation of kinesin's interaction with microtubules. *J. Cell. Biol.* **143,** 1053–1066 (1998).
20. Skoufias, D. A., Cole, D. G., Wedaman, K. P. & Scholey, J. M. The carboxyl-terminal domain of kinesin heavy chain is important for membrane binding. *J. Biol. Chem.* **269,** 1477–1485 (1994).
21. Bi, G. Q. *et al.* Kinesin- and myosin-driven steps of vesicle recruitment for Ca^{2+}-regulated exocytosis. *J. Cell. Biol.* **138,** 999–1008 (1997).
22. Hackney, D. D., Levitt, J. D. & Suhan, J. Kinesin undergoes a 9 S to 6 S conformational transition. *J. Biol. Chem.* **267,** 8696–8701 (1992).
23. Trybus, K. M., Huiatt, T. W. & Lowey, S. A bent monomeric conformation of myosin from smooth muscle. *Proc. Natl Acad. Sci. USA* **79,** 6151–6155 (1982).
24. Trybus, K. M., Freyzon, Y., Faust, L. Z. & Sweeney, H. L. Spare the rod, spoil the regulation: necessity for a myosin rod. *Proc. Natl Acad. Sci. USA* **94,** 48–52 (1997).
25. Kuznetsov, S. A., Vaisberg, Y. A., Rothwell, S. W., Murphy, D. B. & Gelfand, V. I. Isolation of a 45-kDa fragment from the kinesin heavy chain with enhanced ATPase and microtubule-binding activities. *J. Biol. Chem.* **264,** 589–595 (1989).
26. Stewart, R. J., Thaler, J. P. & Goldstein, L. S. Direction of microtubule movement is an intrinsic property of the motor domains of kinesin heavy chain and *Drosophila* ncd protein. *Proc. Natl Acad. Sci. USA* **90,** 5209–5213 (1993).
27. Jiang, M. Y. & Sheetz, M. P. Cargo-activated ATPase activity of kinesin. *Biophys. J.* **68 (suppl.),** 283–284 (1995).
28. Lockhart, A., Crevel, I. M. T. C. & Cross, R. A. Kinesin and ncd bind through a single head to microtubules and compete for a shared MT binding site. *J. Mol. Biol.* **249,** 763–771 (1995).
29. Amos, L. Kinesin from pig brain studied by electron microscopy. *J. Cell Sci.* **87,** 105–111 (1987).
30. Hirokawa, N. *et al.* Submolecular domains of bovine brain kinesin identified by electron microscopy and monoclonal antibody decoration. *Cell* **56,** 867–878 (1989).
31. Lupas, A. Coiled coils: new structures and new functions. *Trends Biochem. Sci.* **21,** 375–382 (1996).
32. Berger, B. *et al.* Predicting coiled coils by use of pairwise residue correlations. *Proc. Natl Acad. Sci. USA* **92,** 8259–8263 (1995).
33. Hancock, W. O. & Howard, J. Processivity of the motor protein kinesin requires two heads. *J. Cell Biol.* **140,** 1395–1405 (1998).
34. Bloomfield, V., Dalton, W. O. & Van Holde, K. E. Frictional coefficients of multisubunit structures. I. Theory. *Biopolymers* **5,** 135–148 (1967).
35. Fersht, A. *Enzyme Structure and Mechanism* (W.H. Freeman, New York, 1985).
36. Hollenbeck, P. J. Phosphorylation of neuronal kinesin heavy and light chains *in vivo*. *J. Neurochem.* **60,** 2265–2275 (1993).
37. Lee, K. D. & Hollenbeck, P. J. Phosphorylation of kinesin *in vivo* correlates with organelle association and neurite outgrowth. *J. Biol. Chem.* **264,** 5600–5605 (1995).
38. Howard, J., Hunt, A. J. & Baek, S. Assay of microtubule movement driven by single kinesin molecules. *Methods Cell Biol.* **39,** 137–147 (1993).

ACKNOWLEDGEMENTS

We thank A. Hunter, P. Detwiler, E. Lumpkin and R. Sawhney for comments on an earlier version of this manuscript. This work was supported by NIH grant AR40593 (to J.H.). D.L.C. was supported by NIH Molecular Biophysics Training Grant GM08268 and by the Achievement Reward for College Scientists. Correspondence and requests for materials should be addressed to J.H. The vectors encoding the following proteins have been deposited at GenBank under the indicated accession numbers: vector pPK113 (kinesin α_2), AF053733; pPK121 (kinesin $\alpha_2\beta_2$), AF055298; pPK115 (Δhinge), AF117643; pH911 (tail-911), AF117644; pPK124 (Δtail), AF161077; p864INS (tail-864), AF116269.